DESIGN OF THE PULSE BENDING MAGNET FOR SWITCHING THE PAINTING AREA BETWEEN THE MLF AND MR IN J-PARC 3-GEV RCS

T.Takayanagi[#], M.Yoshimoto, M.Watanabe, P.K.Saha, T.Ueno, T.Togashi, Y.Yamazaki, M.Kinsho, JAEA/J-PARC, 2-4 Shirakata-Shirane, Tokai, Ibaraki, 319-1195, JAPAN
H.Fujimori, Y.Irie, KEK/J-PARC, 1-1 Oho, Tsukuba, Ibaraki, 305-0801, JAPAN

Abstract

The pulse bending magnet has been designed for switching the painting area between the MLF (Material and Life science Experimental Facility) and MR (50-GeV Main Ring synchrotron) at J-PARC (Japan Proton Accelerator Research Complex) [1]. The pulse magnet is located in injection area of the 3-GeV RCS (Rapid Cycling Synchrotron) [2]-[4]. After upgrading the LINAC (Linear accelerator) beam energy to 400 MeV [5], the two pulse magnets switch the injection beam orbit to change the painting injection area in a pulse-to-pulse mode at 25 Hz. This paper summarizes the design parameters of the pulse bending magnet.

INTRODUCTION

The J-PARC accelerator consists of the 181-MeV LINAC, 3-GeV RCS and MR [1]. In the first stage, the H^- beam from the LINAC at 181 MeV acceleration beam energy has been successfully injected into the RCS and circulated on October 26th in 2008. Furthermore, the acceleration up to the design energy at 3 GeV and the extraction to the beam dump have been achieved on October 31st [2] [3]. In December 7th, 2009, the high power beam demonstration of 300 kW was performed for a period of 1 hour at 25 Hz [4] [6]. The 3-GeV RCS aims at providing at least 300 kW output beam power with the injection beam at 181 MeV. In the second stage, the upgrade of the LINAC beam energy to 400 MeV was funded and started in March 2009. This plan will be completed in 2012 [5]. Consequently, the 3-GeV RCS will aim at 1 MW beam power [7].

The 3-GeV RCS has two functions as a proton beam driver to the spalled neutron source at the MLF and an injector to the MR. However, the required beam parameters for each facility are different. The 3-GeV RCS is designed to satisfy these requirements through changing the painting area in each acceleration cycle. The painting injection in the transverse plane is performed with the pulse bending magnet in the injection line and the injection bump system in the ring [8]-[11].

DESIGNE OF THE PSTR MAGNET

The pulse bending magnet system has the two pulse bending magnets (PSTR01, 02). The PSTRs are located in the L3BT line, which is the injection beam transport line from the LINAC to the 3-GeV RCS. The schematic diagram of the pulse bending magnet system and the injection bump system at the beam injection area of the 3-GeV RCS is shown in Fig. 1.

The PSTR has the purpose to control the injection beam orbit for changing the painting area. For example, the MLF beam painting area is 216 π mm-mrad and the MR beam painting area is 144 π mm-mrad, respectively [12]. Therefore, the operation of the PSTR is changed in every repetition. The injection point at the first foil (FOIL01) can be controlled using two PSTRs and the injection septum magnets (ISEP01, 02) operated by DC excitation. Moreover, the point can be fixed in combination with the PSTR and the bump-magnets. Furthermore, in case of the beam commissioning of the 3-GeV RCS by 400 MeV injection beam, no beam painting (Center Injection) [7] [12] will be performed. Therefore, wide range of the beam deflection angle from 3 mrad to 38 mrad and the uniform magnetic field with less than 1.0 % in homogeneity over a wider area are required (see section 'Specifications').

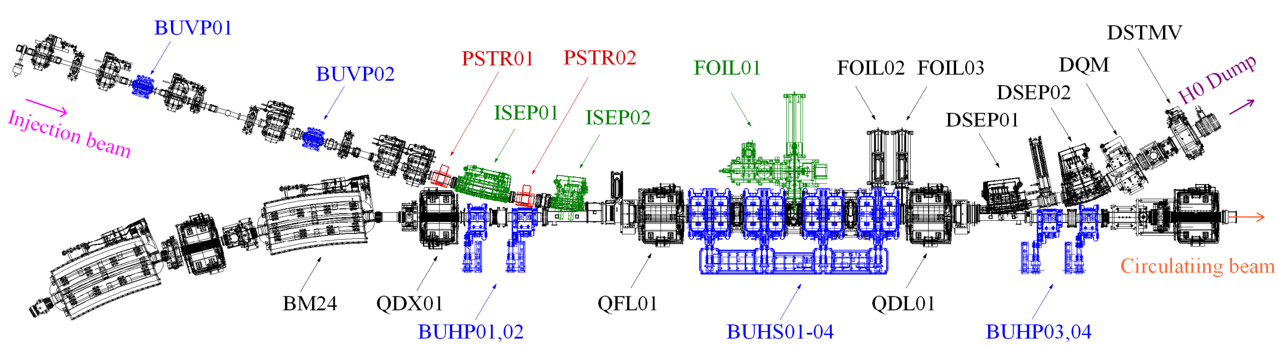

Figure 1: Schematic diagram of the pulse bending magnet system and the injection bump system at the beam injection area of the 3-GeV RCS, which includes two PSTRs, four BUHSs, four BUHPs, two BUVPs and the FOIL01.

tomohiro.takayanagi@j-parc.jp

In the power supply, the flat top time of the excitation current pattern is required to be over 500 μs because of the beam injection. Additionally, the change in 50 % of exciting current is required for switching the painting injection area in a pulse-to-pulse mode at 25 Hz.

Beam stay area

Figure 2 shows the schematic diagram of the cross section of both the beam stay area and the vacuum duct. The beam stay area is the maximum beam size at the entrance and exit of the PSTR. The beam size includes both the beam emittance of 30 π mm-mrad and the beam fluctuation components of 9 mm. The fluctuations take into account β modulation, COD and beam halo [12].

The two PSTRs are located downstream the two BUVPs (see Fig. 1). The BUVP changes the vertical injection angle at the FOIL01. In case of the painting injection (pinj) at 216 π mm-mrad beam emittance, the beam passes over the upper side from a median plane. The maximum displacement is assumed at 20 mm in vertical direction. The PSTR02 is downstream the first injection septum magnet (ISEP01). Therefore, the beam stay area of the PSTR02 is more deflected by the ISEP01. The center injection (cinj) is most close to the side of the duct, which is designed at 93 mm displacement for the shift bump-magnets. The inner size of the ceramic duct is 217 mm in width and 130 mm in height, and the thickness is less than 15 mm with a RF shield [13].

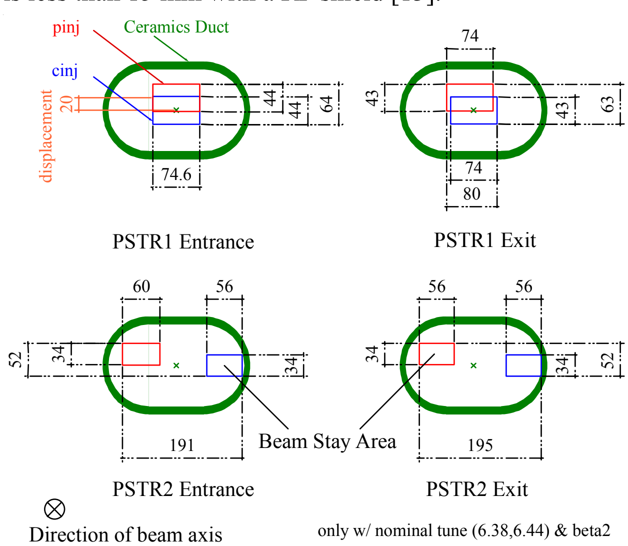

Units : mm

Figure 2: Schematic diagram of the cross section of both the beam stay area and vacuum duct at the entrance and exit of the two PSTRs.

Specifications

The cross section of the magnet and ceramic duct are shown in the Fig. 3, where the total beam stay area, which covers beam size, fluctuations and orbit displacement, amounts to 195 mm in width and 52 mm in height. So the good field region with 1 % in homogeneity of the magnetic field of 208 mm in width and 84 mm in height is necessary.

The design parameters of each magnet and power supply are shown in Table 1. The design of the two PSTRs and each ceramic duct is the same.

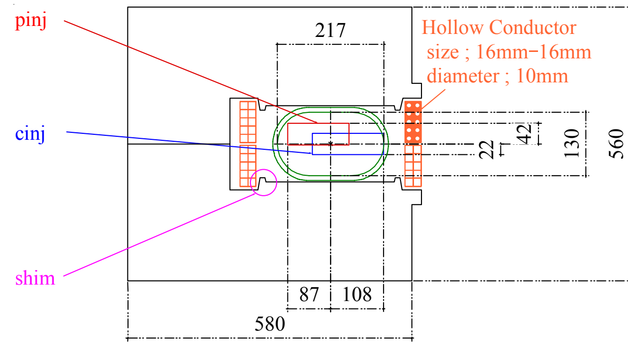

Units : mm

Figure 3: Schematic view of the maximum beam stay area of each beam injection mode and the cross section of magnet, ceramic duct and coil.

Table 1: Parameters of the magnet and the power supply

Contents	Parameter
Magnetic core length [mm]	200
Lamination thickness of the core[mm]	0.35
Magnetic core width/height [mm]	580/560
Gap height[mm]	160
Turns per Coil of the hollow conductor	20
Longitudinal space for installation [mm]	660
Good field region (Horizontal/Vertical) [mm]	208/84
Maximum current for the painting injection [A]	400
Output accuracy of the pulse pattern [%]	0.2
Maximum current for the center injection [A]	3000
Output accuracy of the DC mode [%]	0.01

Magnet

The magnetic core uses the laminated thin steel sheets of 0.35 mm in order to decrease the eddy losses with iron by the pulse operation mode. The laminated core length is 200 mm. The size of the core is 580 mm in width and 560 mm in height. The gap height is 160 mm. The core is divided vertically to install the ceramic duct. The coil uses the hollow conductor with 16 mm square and number of turns is 20. The inner distance of the coil is 304 mm. The longitudinal space for installation is 660 mm.

The installation space of the PSTR is very narrow, as shown in Fig. 4. Especially, the PSTR02 is very close to BUHP02. There is only 43 mm. Therefore, the compact shield with small leakage magnetic field is being designed.

Power supply,

Corresponding to the two modes of the painting injection and the center injection, the exciting current region of the power supply divides into two ranges. In case of the painting injection, the power supply provides the exciting current from 40 A to 400 A, which has the capability to switch from positive to negative polarity. The current pattern becomes a trapezoid pattern by the pulse excitation at 25 Hz. The flat top time is 0.5 ms and both the rise-time and the decay-time are 1.0 ms or longer. So the influence by the eddy current is reduced. In case of the center injection, the exciting current is from 1500 A to 3000 A in DC mode. The power supplies of both the pulse type and the DC type suitable for each specification are produced, separately.

3D simulation of the magnet

The magnetic field analysis of the PSTR has been performed using three-dimensional electromagnetic analysis code, which is ELEKTRA of OPERA-3D [14]. The field analyses for painting and center injections have been performed. The parameters of the exciting current are 400 A at the pulse mode and 1.841 kA at the DC mode. Analysis results of the integrated magnetic field distribution of each mode are shown in Figs. 5 and 6.

By optimizing the design of the core with the shim and the coil, a wide uniform magnetic field with less than 1.0 % inhomogeneous distribution has been achieved. No field saturation is seen in this excitation level, although it can be observed above 2400 A.

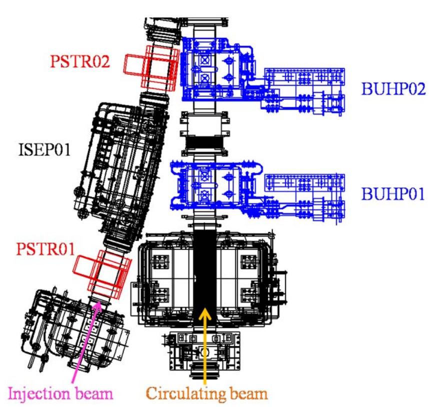

Figure 4: Schematic of the installation space of the PSTR.

CONCLUSION

The PSTR has realized a uniform field with less than 1.0 % in homogeneity over a wider area, which has high proportion of gap (160 mm) versus core length (200 mm). Both the magnets and the power supplies will be produced in this fiscal year, 2010, and the magnetic field of the PSTR will be measured by using the power supply in the laboratory in the next year. The installation of these machines will be performed in 2012.

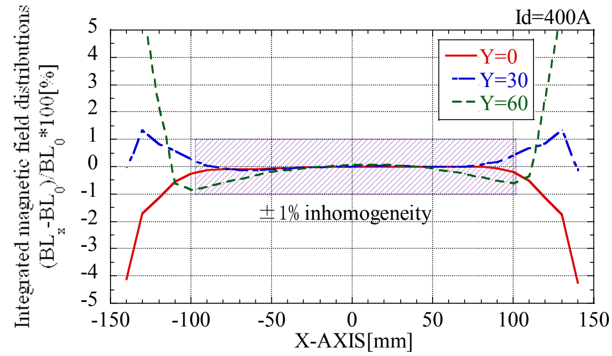

Figure 5: Magnetic field analysis result of the 400 A of the pulse mode with the painting injection.

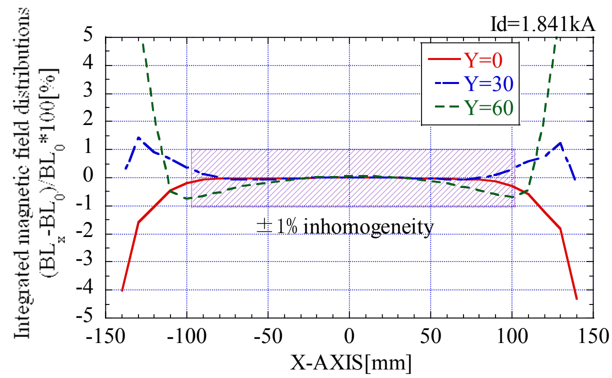

Figure 6: Magnetic field analysis result of the 1.841 kA of the DC mode with the center injection.

REFERENCES

[1] KEK Report 99-4 and JAERI-Tech 99-056 (1999).
[2] M. Kinsho, Proceedings of EPAC08, Genoa, Italy, THXG02, p. 2897 (2008).
[3] M. Kinsho, Proceedings of PAC09, Vancouver, BC, Canada, TU6PFP065.
[4] M. Kinsho, IPAC'10, MOPEC069.
[5] N.Ouchi, Proceedings of SRF2009, Berlin, Germany, FROBAU05, p.934 (2009)
[6] H. Hotchi, IPAC'10, MOPEC068.
[7] H. Hotchi, et al., Proceedings of PAC09, Vancouver, BC, Canada, TU6PFP090
[8] T. Takayanagi, et al., Proceedings of PAC05, Knoxville, Tennessee, P.1040(2005)
[9] T. Takayanagi, et al., IEEE Transactions on Applied Supercond., vol.16, no.2, pp.1358-1361, June. 2006
[10] T. Takayanagi, et al., IEEE Transactions on Applied Supercond., vol.18, no.2, pp.310-313, June. 2008
[11] T. Takayanagi, et al., Proceedings of PAC09, Vancouver, BC, Canada, TU6PFP083
[12] P.K. Saha, et al., Physical Review Special Topics, Accelerator and beams 12, 040403 (2009)
[13] M. Kinsho, et al., Vacuum, 73, 2004, pp.187-193.
[14] Vector Fields Software